A Multifunctional Tripodal Fluorescent Probe for the Recognition of Cr³⁺, Al³⁺, Zn²⁺ and F⁻ with Controllable ESIPT Processes†

Hong Zhang,[a] Tao Sun,[e] Qin Ruan,[a] Jiang-Lin Zhao,*[b] Lan Mu,[a] Xi Zeng,*[a] Zongwen Jin,*[b] Shaobo Su,[b] Qingying Luo,[b] Yiyong Yan[c] and Carl Redshaw[d]

Three 4-(benzo[d]thiazol-2-yl)-2,5-dihydroxybenzaldehyde fluorophores were introduced to construct a tripodal multifunctional ESPIT fluorescence probe **L**. The fluorescent analysis revealed that probe **L** exhibited excellent recognition capability towards Cr³⁺, Al³⁺, Zn²⁺ and F⁻ ions with large Stokes shift. Furthermore, under the optimal conditions, the detection limit of probe **L** towards Cr³⁺, Al³⁺, Zn²⁺ and F⁻ were low, of the order of 10^{-8} M, which indicated that probe **L** was sensitive to these four ions. Interestingly, the fluorescent and ¹H NMR titration experiments revealed that the recognition mechanism of probe **L** towards the ions Cr³⁺, Al³⁺, Zn²⁺ and F⁻ were different. The presence of Cr³⁺ and Al³⁺ recovered the ESIPT, but the presence of Zn²⁺ trigger a moderate deprotonation of the phenolic OH and induced an ESIPT red shifted (60nm) emission wavelength. Finally, the presence of F⁻ completely deprotonated the free phenolic OH and a remarkable red shifted (130 nm) ESPIT emission was observed. In other words, the ESIPT process of probe **L** is controllable. Furthermore, the utility of probe **L** as a biosensor in living cells (PC3 cells) towards Cr³⁺, Al³⁺ and Zn²⁺ ions has been demonstrated.

Keywords
Fluorescent probe
ESIPT
Recongnition
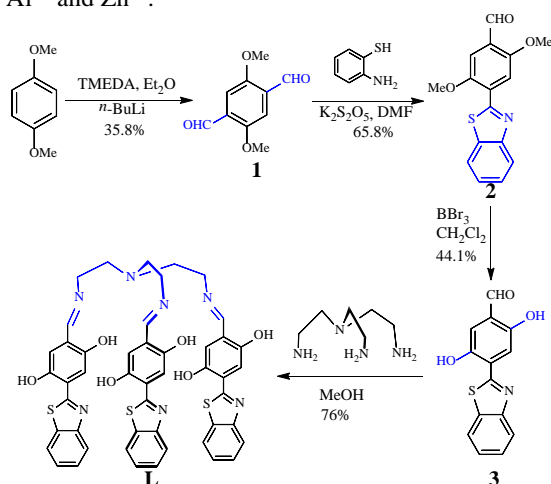Cr³⁺, Al³⁺, Zn²⁺ and F⁻
Living cell

1. Introduction

Fluorescent probe assays have been studied for many years due to their high sensitivity, selectivity, real-time imaging and ease of manipulation.[1] Using both the literature and our own experience, there are a number of interesting phenomenon which can help guide the design of a fluorescent probe. For example, the fluorescence "turn on" probe is normally better than the "turn off" probe given the associated low background interference.[2] Secondly, a larger Stokes shift and higher sensitivity for a fluorescent probe can be achieved by reducing self-quenching and auto-fluorescence, which results from minimal overlap of the excitation and emission spectra.[3] Thirdly, ratiometric fluorescent probes are accurate as they measure the observed changes in the ratio of the intensities of the emission at two wavelengths, which provides a built-in correction for environmental effects. In other words, they are not influenced by the microenvironment, probe concentration, photobleaching, excitation intensity, and so on.[4]

4-(Benzothiazol-2-yl)phenol and its derivatives are good probe candidates as they possess the above advantages. As fluorophores, they have many excellent photophysical and photochemical characteristics such as a relatively high fluorescent quantum yield and good cell membrane permeability.[5] Meanwhile, their ease of synthetic modification

and good photostability are also attractive attributes. Further, they can exhibit dual emission *via* the excited state intramolecular proton transfer (ESIPT) processes upon being excited, which means they can be developed as ratiometric probes.[5a,6]

Considering all of this, 4-(benzothiazol-2-yl)phenol seems to be an ideal fluorophore for constructing an efficient multifunctional fluorescent probe. Indeed, a number of excellent fluorescent probes have been explored which contain one benzothiazole moiety as a fluorophore.[6c,7] However, how about if we introduce more than one benzothiazole fluorophore? Will its properties be better? Herein, we have designed and synthesized a tripodal fluorescent probe **L** by introducing three 4-(benzothiazol-2-yl)phenols as the ESIPT fluorophore. Impressively, probe **L** exhibited excellent recognition capability towards the ions Cr³⁺, Al³⁺, Zn²⁺ and F⁻. More interestingly, it was found that the ESIPT emission wavelength of probe **L** can readily be controlled by the above mentioned ions. Besides, the good cell membrane permeability of probe **L** makes it a potential biosensor in living cells for the detection of Cr³⁺, Al³⁺ and Zn²⁺.

Scheme 1 The synthetic route of probe **L**.

2. Results and discussion

2.1. Synthesis

The tripodal fluorescence probe **L** was obtained by the convenient condensation of tren and three equivalents of 4-(benzo[*d*]thiazol-2-yl)-2,5-dihydroxybenzaldehyde (**3**) in one step (Scheme 1). Its structure was fully characterized by IR, ^{1}H NMR and ^{13}C NMR spectroscopy and MS. The proton signal of the precursor **3** aldehyde group hydrogen disappeared, whilst a new singlet appeared at about 8.22 ppm, which is attributed to the formation of the CH=N linkage of the Schiff base skeleton in probe **L**. Besides, the appearance of two new triplets at 3.69 and 2.93 ppm is associated with the methylene group of the tren moiety further confirming the success of the condensation reaction (for details, see the Supporting Information, Fig. S20-S23).

### 2.2. Recognition properties of probe L towards metal ions

The recognition properties of probe **L** were investigated by fluorescence spectroscopy. In DMF/H$_2$O (v/v = 96/4, Tris-HCl buffer, pH = 7) solution, probe **L** (10 μM) exhibited a weak emission at about 480 nm (λ_{ex} = 320 nm), which is attributed to the *keto* emission generated from the excited-state intramolecular proton transferred (ESIPT) process in probe **L**.[5c,7a] However, fast C=N isomerization was the predominant decay process for the excited state of probe **L**, and this greatly diminished the emission intensity at 480 nm.[8] Hence, we only observed a weak fluorescent emission for probe **L** at 480 nm (Fig. 1a). In other words, the ESIPT process was greatly affected (adversely) by the presence of the Schiff base group in **L**. Interestingly, upon addition of Cr^{3+} and Al^{3+}, an acute fluorescence enhancement at 480 nm with a large Stokes shift (160 nm) was observed. This is ascribed to the formation of the **L**-Cr^{3+} or **L**-Al^{3+} complexes inhibiting the C=N isomerization of probe **L**. Besides, the addition of Zn^{2+} ion not only induced an enhancement at 480 nm but also a new emission peak appeared at 540 nm, which indicated a different recognition pathway for probe **L** towards Zn^{2+}. In contrast, the presence of any other metal ions did not bring about significant fluorescence changes, which indicated the higher selectivity of probe **L** towards Cr^{3+}, Al^{3+} with Zn^{2+}. Furthermore, the two different wavelength responses are accompanied by two different colour changes (cyan and a yellow/green colour, Fig. 1a inset) enabling probe **L** to possess the capability to further differentiate between Cr^{3+}, Al^{3+} *versus* Zn^{2+} by the naked eye.

In order to investigate the detailed recognition processes, fluorescent titration experiments were carried out. Upon increasing the concentration of Cr^{3+}, only a fluorescence enhancement at 480 nm (Stokes shift =160 nm) was observed, which reached equilibrium upon addition of about 1.0 equivalent of Cr^{3+}. This suggested a 1:1 binding ratio (the quantum yield Φ = 0.36 *versus* quinine sulfate as reference material, Φ = 0.55, Fig.1b). Similar phenomena were observed upon the addition of Al^{3+} (Φ = 0.35, Fig. S1). It should be noted that a large Stokes shift (Stokes shift > 100 nm) normally indicates that the ESIPT process has occurred. The enhancement of the fluorescence band at 480 nm indicated the suppression of C=N isomerization and the recovery of the ESIPT process. Interestingly, upon addition of Zn^{2+}, the fluorescence significantly increased, and not only gave an emission at 480 nm but also observed at 540 nm
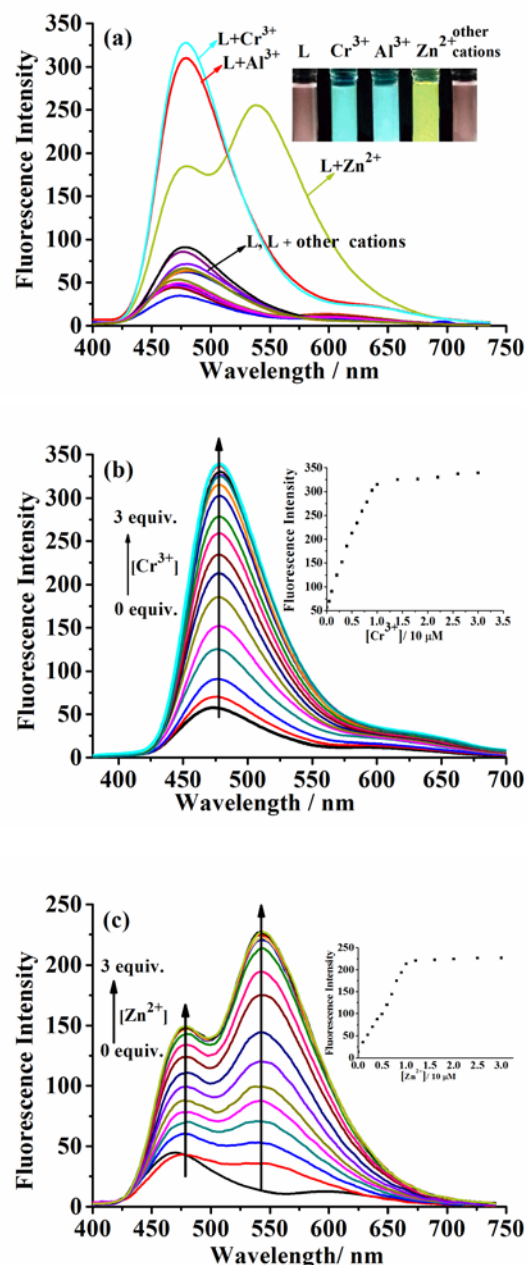
Figure 1. (a) Fluorescence spectra of probe **L** (10 μM, DMF/H$_2$O, v/v = 96/4, pH = 7) without or with 20 equiv. of the various metal ions. Inset: the colour changes of probe **L** in the absence and the presence of Cr^{3+}, Al^{3+} or Zn^{2+} under UV-vis light; (b) Fluorescence spectral changes of probe **L** (10 μM, DMF/H$_2$O, v/v, 96/4, pH 7) solution upon addition of Cr^{3+} or (c) Zn^{2+} (0 ~ 30 μM). Inset: the plot of fluorescence intensity of probe **L** as a function of Cr^{3+} or Zn^{2+} concentration. Cations include Li$^+$, Na$^+$, K$^+$, Ag$^+$, Mg^{2+}, Ca^{2+}, Ba^{2+}, Sr^{2+}, Hg^{2+}, Co^{2+}, Ni^{2+}, Cu^{2+}, Pb^{2+}, Cd^{2+}, Mn^{2+}, Zn^{2+}, Fe^{3+}, Cr^{3+}, Al^{3+}, λ_{ex} = 320 nm.

(Stokes shift = 220 nm) was a fluorescent emission (Φ = 0.38, Fig. 1c). The emission at 480 nm belonged to the ESIPT "on" of probe **L**, while the stronger fluorescence at the longer wavelength (540 nm) was associated with the deprotonation of Ph-OH / Ph-O$^-$ which further enhanced the electron donating
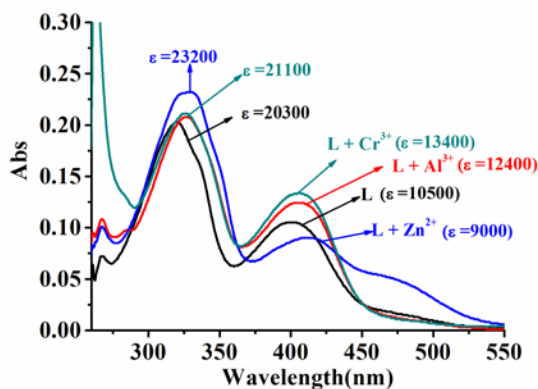
Figure 2. Absorption spectra of probe **L** (10 μM, DMF/H₂O, v/v = 96/4) without or with 20 equiv. Cr³⁺, Al³⁺ or Zn²⁺.

ability of the phenolic O⁻ toward the benzothiazole core acceptor[9]. This system also reached equilibrium upon the addition of 1.0 equivalent of Zn²⁺ ion (Fig. 1c inset). The Cr³⁺/Al³⁺ ions only induced an enhanced emission at 480 nm, which is tentatively attributed to a weak interaction of the Cr³⁺/Al³⁺ ions with the imine -CH=N- and adjacent hydroxyl groups. As a result, the system could not remove the phenolic proton (a necessary step for the emission shift)[9].

To elucidate the metal ion-binding mode present, the UV-vis spectra of probe **L** in the presence of Cr³⁺, Al³⁺ or Zn²⁺ were investigated. The absorption of probe **L** exhibited a major peak at 320 nm (π-π*) and a minor peak at 400 nm (n-π*) (Fig. 2). Upon the addition of Al³⁺ and Cr³⁺, both of the absorption intensities at 320 nm and 400 nm were enhanced which indicated the formation of **L**-Cr³⁺ or **L**-Al³⁺ complexes. However, no significant bathochromic shifts in the absorption spectra were observed in the presence of Al³⁺ and Cr³⁺ which suggested weak binding of the Al³⁺ and Cr³⁺ ions with the -CH=N- moiety and it's adjacent phenol. In other words, the presence of Al³⁺ and Cr³⁺ cannot remove the phenolic proton of probe **L**. Contrastingly, when Zn²⁺ ions were added, the absorption band at 328 nm increased, but the n-π* absorption band at 400 nm decreased and shifted to 415 nm which indicated that the Zn²⁺ ion was bonded to the Schiff base. A new (π-π*) absorption band was simultaneously generated at about 475 nm which was attributed to the removal of a phenolic proton required for the formation of the **L**²⁻-Zn²⁺ complex. The UV results are consistent with the fluorescence spectra analysis.

The ¹H NMR titration experiments gave further insight into the possible recognition mechanism. Upon increasing the concentration of Cr³⁺, a remarkable up-field chemical shift of the OH proton (H_{11}) was observed. Meanwhile, the singlet protons of the imine (H_3) were converted to triplets and slightly shifted downfield, which indicated this OH and the imine N atoms participated in the recognition of Cr³⁺ (Fig. 3a). Consequently, the adjacent protons (H_4 and H_{10}) were effected and were shifted downfield. Due to the complexation of Cr³⁺, the nature of the structure of probe **L** was fixed, and the C=N isomerization of probe **L** was inhibited. Hence, the fluorescence of probe **L** was switched on which is consistent with the fluorescent result. However, no significant chemical shift
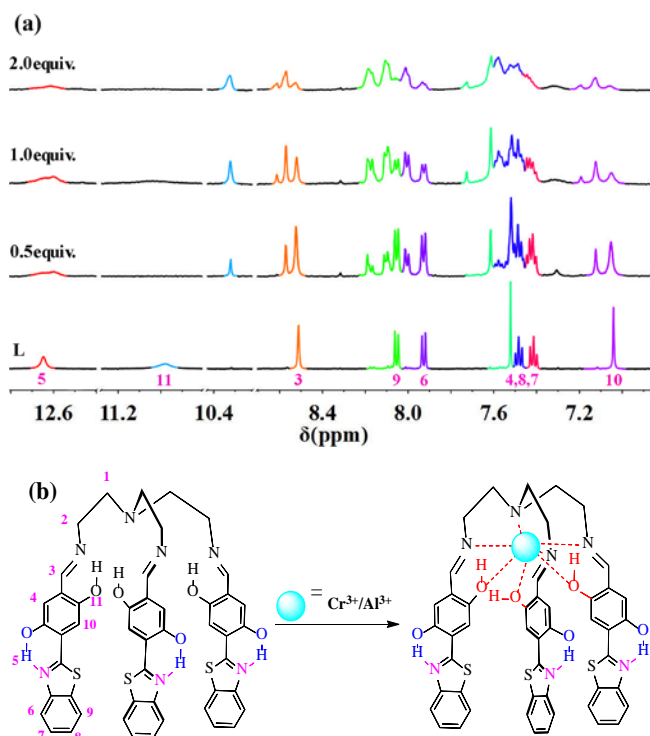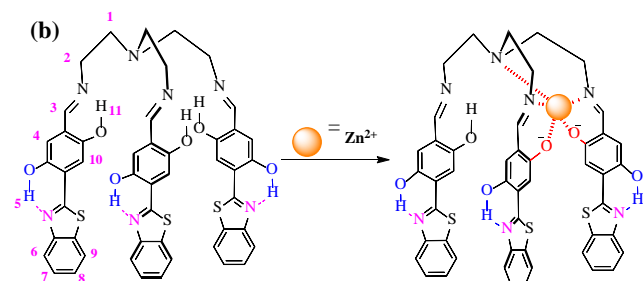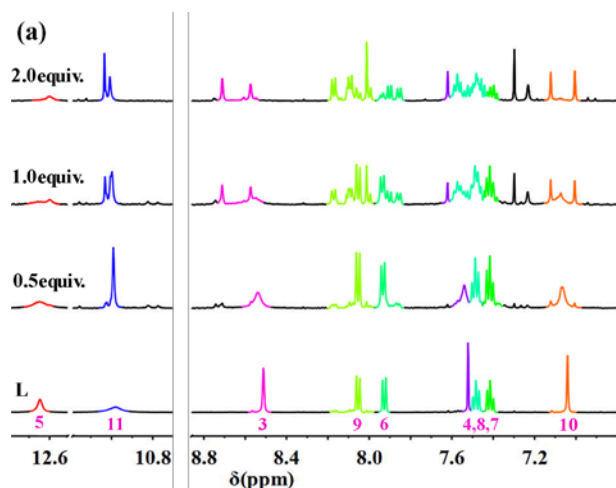

Figure 3. (a) Partial ¹H NMR spectra of probe **L** (5.0 mM) and increasing concentrations of Cr³⁺ in DMSO-*d6* at 298K; (b) Plausible recognition mechanism of the probe **L** towards Cr³⁺/Al³⁺.

changes for the benzothiazol protons (H_6, H_7, H_8 & H_9) were observed which means the binding site is far removed from the benzothiazol moiety. Similar phenomena were observed in the case of Al³⁺, which suggested the same recognition mechanism for Cr³⁺ and Al³⁺. The Job's plot analysis revealed a 1:1 binding stoichiometry for probe **L** towards Cr³⁺ or Al³⁺ (Fig. S2), and the 1:1 nature of the **L**-Cr³⁺ and **L**-Al³⁺ complexes was further confirmed by MALDI-TOF mass spectrometry. The difference of the mass charge ratio between the mass peaks at *m/z* 930.804 (calculated value 930.178), 931.843 and 932.718 were about 1, which means [**L**+Al-2H]⁺ was a single charged isotopic peak. Similarly, the difference of mass charge ratio between mass peaks at *m/z* 958.552 (calculated value 958.161), 959.606, and 960.772 were about 1, which means [**L**+Cr+H]⁺ was also a singly charged isotopic peak. All the results indicated the formation of 1:1 complexes of the type **L**-Al³⁺ and **L**-Cr³⁺ (Fig. S3 & S4). Combining all of the above observations, a plausible recognition mechanism for the probe **L** towards Cr³⁺/Al³⁺ is shown in Fig. 3b.

On the other hand, the ¹H NMR titration experiments involving Zn²⁺ (Fig. 4a), revealed obvious differences compared with the addition of Cr³⁺/Al³⁺. Upon addition of Zn²⁺, the proton signal of OH (H_{11}) was split into two peaks, and at the same time, the imine H_3 (at δ 8.51 ppm) was also split into two peaks and shifted downfield to about δ 8.57 & 8.71 ppm. This suggested that both the imine and hydroxyl groups participated in the complexation process with Zn²⁺. Noteworthy, in the presence of Zn²⁺, the Schiff base proton (H_3) and the hydroxyl protons were clearly split into two, and the ratio was about ~ 2:1. The two kinds of proton signal for the Schiff base and

OH were ascribed

Figure 4. (a) Partial ^{1}H NMR spectra of probe **L** (5.0 mM) and increasing concentrations of Zn^{2+} in DMSO-*d6* at 298K; (b) Plausible recognition mechanism of the probe **L** towards Zn^{2+}.

to the presence of two kinds of imine moieties and hydroxyl groups for probe **L**, *viz.* one participates in the complexation, the other does not. A 1:1 binding stoichiometry for the **L**-Zn^{2+} complex was further confirmed by mass spectrometry. The mass peak at *m/z* 969.231 (calculated value 969.142) and other isotope peaks were observed which corresponded to a singly charged isotope [**L**+Zn+H]$^+$ strongly suggestive of the formation of a 1:1 complex (Fig. S5). Consequently, combined with the UV and fluorescence results, we proposed the binding mechanism shown in Fig. 4b. This binding mechanism for Cr^{3+}, Al^{3+} and Zn^{2+} was further supported by the computational study (Figs. S6 & S7).

2.3. Recognition properties of probe L towards F$^-$

For the recognition properties of probe **L** towards anions, we found that probe **L** exhibited a high selectivity towards F$^-$ in 1,4-dioxane solution by using the fluorescence method. Upon the addition of 10 equiv. of various anions (F$^-$, Cl$^-$, Br$^-$, I$^-$, PF$_6^-$, NO$_3^-$, H$_2$PO$_4^-$, HSO$_4^-$, AcO$^-$, ClO$_4^-$), only the presence of F$^-$ induced a dramatically ratio metric change and resulted in a remarkable colour change which enable us to distinguish F$^-$ by the naked eye (Φ = 0.19, Fig. 5a). Although there were some slight spectral changes in the presence of AcO$^-$ and H$_2$PO$_4^-$, it proved too difficult to utilize this system for practical application in the detection of these two anions due to the near lack of fluorescence.

The fluorescent titration experiments provided information relating to the recognition process. Upon increasing the concentration of F$^-$, the emission at 480 nm gradually decreased, whilst the emission at 610 nm increased with an isobestic point at
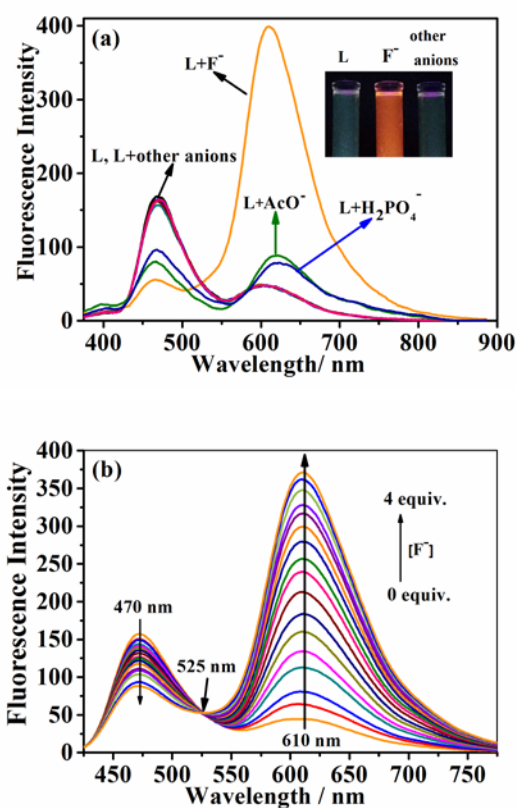
Figure 5. (a) Fluorescence spectra of probe **L** (40 μM, 1,4-dioxane) without or with 10 equiv. of various anions (inset shows the colour change of probe **L** in the absence and the presence of F$^-$ under UV-vis light.); (b) Fluorescence spectral changes of probe **L** (40 μM, 1,4-dioxane) solution upon addition of F$^-$ (0 ~ 160 μM). λ_{ex} = 350 nm.

525 nm (the Stokes shift is higher than 260 nm, Fig. 5b) which indicated probe **L** can serve as a ratiometric fluorescent probe for F$^-$. The remarkable red shifted emission can be attributed to the F$^-$ induced deprotonation of a phenolic OH (H_{11}) which is adjacent to the Schiff base bond in probe **L**.[10] The mol ratio method and Job's plot suggested a 1:1 binding stoichiometry for probe **L** towards F$^-$ (Fig. S8). We further employed ^{1}H NMR spectroscopic titrations to try and elucidate the binding mechanism of F$^-$ (Fig. 6a). Due to the poor solubility of probe **L** in 1,4-dioxane, we conducted the ^{1}H

NMR spectroscopic titration experiments in DMSO solution. Upon the addition of F$^-$, the proton signals of OH (H_5 & H_{11}) disappeared and remarkable chemical shifts for the protons (H_4 & H_{10}) in the phenolic ring and the adjacent Schiff base proton (H_3) were observed. However, no significant chemical shift changes for the other protons (the benzothiazol moiety, H_6, H_7, H_8 & H_9) were observed. All of the observations further supported the suggestion that the F$^-$ anion was interacting with the phenolic moiety of probe **L**, *via* deprotonation of the phenolic OH. Binding with fluoride is probably driven by processes associated with hydrogen bond formation and deprotonation, and are attributed to the basicity of the fluoride anion and its strong ability to form hydrogen bonds. The occurrence of this process further enhanced the electron donating ability of the phenolic O$^-$ to the thiazole core acceptor, resulting in an intramolecular charge transfer process.[11] With this in mind, a
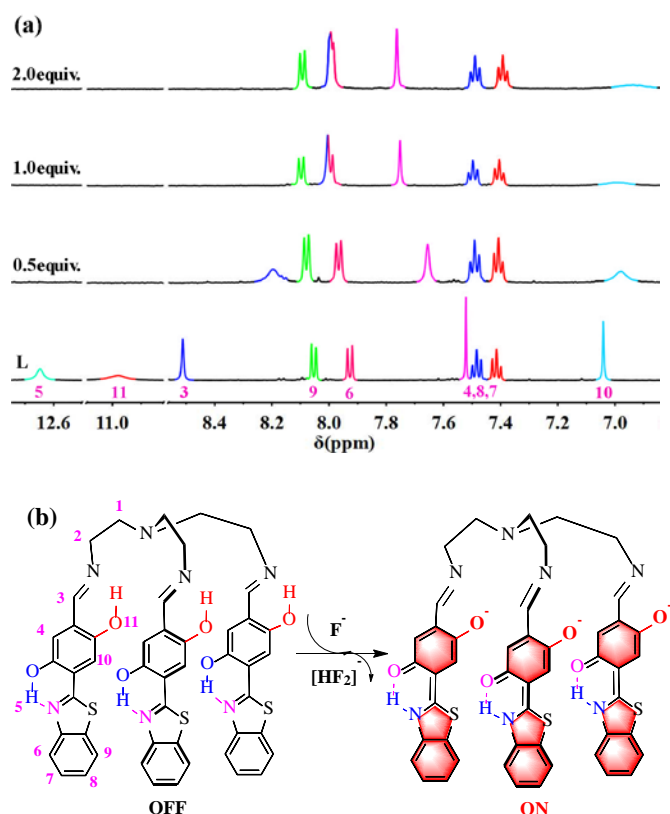
Figure 6. (a) Partial ^{1}H NMR spectra of probe **L** (5.0 mM) and increasing concentrations of F$^-$ in DMSO-*d6* at 298K; (b) Plausible recognition mechanism of the probe **L** towards F$^-$.

possible recognition mechanism for probe **L** towards F$^-$ is shown in Figure 6b.

Competitive experiments were carried out to investigate the practical applicability of probe **L** as a Cr^{3+} or Al^{3+} or F$^-$ ion selective fluorescent probe. There was no obvious interference to the selective response of probe **L** towards Cr^{3+} or Al^{3+} or F$^-$ ions in the presence of most of the other ions screened (Fig. S9) which suggested a high selectivity for probe **L**. Under the optimal conditions, a linear range for the calibration curve was detected; binding constants and limits of detection (LOD = 3σ /slope) for probe **L** with Cr^{3+}, Al^{3+}, Zn^{2+} and F$^-$ are summarized in Table 1. The larger binding constant indicates the stable nature of the complex of probe **L** with Cr^{3+}, Al^{3+}, Zn^{2+} and F$^-$. All of the LODs for probe **L** towards Cr^{3+}, Al^{3+}, Zn^{2+} and F$^-$ were of the order of 10^{-8} M by fluorescence, which indicated that probe **L** is sensitive to these four ions.

The high selectivity of probe **L** towards Cr^{3+}, Al^{3+} and Zn^{2+} may depend on the unique molecular structure of probe **L**. The three flexible chains of probe **L** not only participate in the coordination action of ions, but also provide some special shielding effects due to the bulky 3D nature of the structure, which can further improve the selectivity. The ^{1}H NMR titration analysis and the density function theory calculations revealed that only two flexible chains of probe **L** participate in the coordination with Zn^{2+}, and that the configuration of probe **L**-Zn^{2+} complex is a partial cone structure. By contrast, the configurations of probes **L**-Al^{3+} and **L**-Cr^{3+} are a cone structure due to the three flexible chains of probe **L** participating in the coordination. The cooperation of coordination and spatial effects of probe **L** are the key factors dictating the recognition ability towards different ions.

The sensitivity of probe **L** towards Cr^{3+}, Al^{3+} and Zn^{2+} may also be due to the presence of the benzothiazole moiety which possesses the ESIPT ability and high quantum yields. Herein, we introduced three benzothiazole moieties as fluorophores which greatly enhanced the fluorescent intensity and also can improve the sensitivity.

2.5. Cell imaging study

The capability of probe **L** to monitor Cr^{3+}, Al^{3+} and Zn^{2+} ions within living cells was investigated by fluorescence imaging on an inverted fluorescence microscope. Given their emission wavelength, for Cr^{3+} and Al^{3+}, the optical window at the blue channel was chosen as a signal output; for the Zn^{2+}, the optical windows at the green and red channel were chosen as a signal output. After incubation of the PC3 cells with 20 μM of probe **L** for a pre-longed period, the cells were still alive (bright-field image, Fig. 7a) which indicated that probe **L** exhibited low toxicity. Cytotoxicity was further confirmed by using MTT (3-(4,5-dimethylthiazol-2-yl)-2,5-diphenyltetrazolium bromide) assays. It was performed by

Table 1 Analysis parameters for probe **L** and detection of Cr^{3+}, Al^{3+}, Zn^{2+} and F$^-$.

Ion	Solvent	$\lambda_{ex}/\lambda_{em}$ (nm)	The linear range of the calibration curve (μM)	Correlation coefficient	Limits of detection ($\times 10^{-8}$ M)	Binding constant (M^{-1})
Cr^{3+}	DMF/H$_2$O	320/480	0.5~ 10	0.98773 (n = 12)	2.5	1.9905×10^7

Al^{3+}	DMF/H_2O	320/480	$1.0 \sim 10$	0.99657(n = 11)	2.7	4.8576×10^6
Zn^{2+}	DMF/H_2O	320/540	$1.0 \sim 10$	0.99657(n = 11)	3.3	3.0971×10^7
F^-	1,4-dioxane	350/(610/470)	$4 \sim 40$	0.99266 (n = 11)	6.7	1.2374×10^5
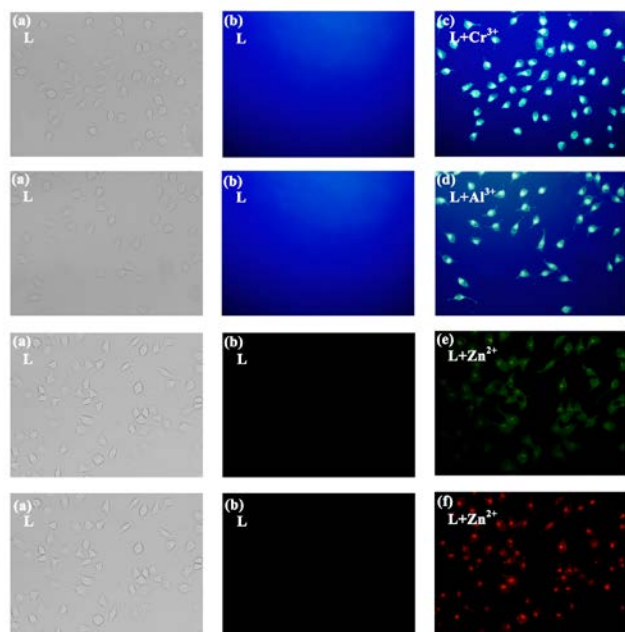
Figure. 7 Fluorescence images of PC3 cells: (a) bright-field image of cells after incubation with probe **L** (20 μM); (b) fluorescence image of (a); (c) and (d) fluorescence image of probe **L** on further treatment with cells after incubation with Cr^{3+} and Al^{3+} (100 μM) solution in the blue channel; (e) and (f) fluorescence image of probe **L** on further treatment of cells after incubation with Zn^{2+} (100 μM) solution in the green channel or red channel.

directly determining the effect of probe **L** on the cellular viability of MCF-7 under our laboratory conditions. The MCF-7 was either treated with different concentrations of probe **L** (10, 50, 100 and 500μM) or left untreated as a control. The results showed that probe **L** at the concentrations 0, 10, 50, 100 and 500μM had no significant effect on cell viability over about 60 minutes (Fig. S10).

As expected, almost no intracellular fluorescence was observed in the fluorescence image due to the non-fluorescence of probe **L** (Fig. 7b). The incubated cells were then treated with Cr^{3+}, Al^{3+} or Zn^{2+} for about 50 min,., whereupon a remarkable intracellular fluorescence was triggered (Fig. 7c~7f). It unambiguously indicated that the remarkable fluorescence was induced by the response of probe **L** towards intracellular Cr^{3+}, Al^{3+} or Zn^{2+}. These results strongly suggest that probe **L** can penetrate the cell membrane and can monitor intracellular Cr^{3+}, Al^{3+} and Zn^{2+} in PC3 cells by *in vitro* imaging. There is also the potential to utilize **L** for *in vivo* methods.

3. Conclusions

A tripodal multifunctional fluorescence probe **L** was synthesized in one-step and high yield by the convenient condensation of tren and three equivalents of 4-(benzo[*d*]thiazol-2-yl)-2,5-dihydroxybenzaldehyde. The presence of the benzothiazol moiety allows probe **L** to possess ESPIT capability. The fluorescent analysis revealed that probe **L** not only exhibited excellent recognition capability towards Cr^{3+}, Al^{3+}, Zn^{2+} and F^- ions with a large Stokes shift, but also possessed a low detection limit, which is of the order of 10^{-8} M towards these four ions. The UV analysis, fluorescent and ^1H NMR spectroscopic titration experiments revealed information about the recognition mechanism of probe **L** towards Cr^{3+}, Al^{3+}, Zn^{2+} and F^- : namely probe **L** exhibited a weak emission at about 480 nm due to fast C=N isomerization which inhibited the ESIPT process. Furthermore, the introduction of either Cr^{3+} or Al^{3+} can suppress the C=N isomerization and lead to recovery of the ESPIT process, which in-turn results in the fluorescence enhancement at 480 nm. Whilst the presence of Zn^{2+} can trigger some deprotonation of the phenolic OH leading to an ESIPT emission red shift (60 nm) to 540 nm, the addition of F^- can completely deprotonate the free phenolic OH and result in a remarkable ESPIT emission red shift (130 nm) to 610 nm. In other words, the ESPIT process of probe **L** is controllable by addition of Cr^{3+}, Al^{3+}, Zn^{2+} and F^-. Probe **L** have also demonstrated that it has low toxicity and can serve as a biosensor in living cells (PC3 cells) towards Cr^{3+}, Al^{3+} and Zn^{2+} ions.

4. Experimental

4.1. Materials and methods

Unless otherwise stated, all reagents used were purchased from commercial sources and were used without further purification. The solutions of the metal ions were prepared from their perchlorate salts (Aldrich and Alfa Aesar Chemical Co., Ltd.). All the anions used were tetra-*n*-butylammonium salts (Sigma-Aldrich Chemical Co., Ltd.), and were stored in a desiccator under vacuum containing self-indicating silica. Double distilled water was used throughout. Fluorescence spectral measurements were performed on a Cary Eclipse fluorescence spectrophotometer (Agilent Technologies) equipped with a xenon discharge lamp using a 1 cm quartz cell. UV-Vis absorption spectra were conducted on a UV-1800 spectrophotometer (Shimadzu) in a 1 cm quartz cell. IR spectra were obtained using a Vertex 70 FT-IR spectrometer (Bruker). ^1H and ^{13}C NMR spectra were measured on a JEOL JNM-ECZ400S 400 MHz NMR spectrometer (JEOL) and a WNMR-I 500 MHz NMR spectrometer respectively at room

temperature using TMS as an internal standard. MALDI-TOF mass spectra were measured on an AB SCIEX TripleTOF^{AM} ^{5600} system. Microelectrode layers used the sputtering and lift-off process with the standard photo-lithography (EVG 610, Austria). Cell fluorescence imaging was performed using a Ti (Nikon) fluorescent inverted phase contrast microscope.

4.2. Synthetic of intermediate 1

A mixture of *p*-dimethoxybenzene (5.52 g, 40 mmol), tetramethylethylenediamine (TMEDA, 30 mL, 200 mmol) and dry ether (140 mL) were cooled to 0 °C in an ice bath under an N$_2$ atmosphere. *n*-Butyllithium (100 mL, 160 mmol) was then slowly added into the above solution. The mixture was stirred for a further 10 min at 0 °C, and then it was heated up to reflux for 20 h. After cooling the reaction mixture to room temperature, 17.2 mL DMF (220 mmol) was added. The mixture was further stirred at r.t. overnight. 100 mL water was added to quench the reaction. The product was extracted with chloroform (100 mL × 3) three times, washed with water (60 mL × 2) and dried with anhydrous Mg$_2$SO$_4$. The crude product was obtained by vacuum rotary evaporation to remove organic solvents. The desired intermediate **1** was purified by column chromatography (*n*-hexane/toluene, 6/4, v/v, silica gel) to give a yellow solid in 35.8 % yield. m.p. 151.9 ~ 152.7 °C. ^{1}H NMR (400 MHz, CDCl$_3$) δ: 10.50 (s, 2 H, -C*H*O), 7.46 (S, 2 H, Ar*H*) and 3.95 (s, 6 H, -OC*H*$_3$) ppm; ^{13}C NMR (400 MHz, CDCl$_3$) δ: 189.35, 155.80, 129.17, 110.96 and 56.29 ppm. MS (ESI) *m/z*: calcd for C$_{10}$H$_{10}$O$_4$, 194.1, Found 195.2 [M + H]$^+$ and 217.2 [M + Na]$^+$.

4.3. Synthetic of intermediate 2

A mixture of intermediate **1** (4.2 g, 21.65 mmol), 2-aminothiophenol (2.36 g, 21.65 mmol) and potassium metabisulphite (5.3 g, 23.84 mmol) in DMF (150 mL) was refluxed for 3h under an N$_2$ atmosphere. After the mixture was cooled to room temperature, it was poured into ice-water (250 ml) to afford a yellow precipitate, which was isolated (filtration) and further purified by silica gel chromatography using CH$_2$Cl$_2$ as eluent to give 4.25 g of a yellow powder **2** in 65.8 % yield. m.p. 172.3 ~ 173.5 °C. ^{1}H NMR (500 MHz, CDCl$_3$) δ: 10.52 (s, 1 H, -C*H*O), 8.27 (s, 1 H, Ar*H*), 8.13 (d, *J* = 8.0 Hz, 1 H, Ar*H*), 7.96 (d, *J* = 7.0 Hz, 1 H, Ar*H*), 7.52 ~ 7.55 (m, 2 H, Ar*H*), 7.43 (t, *J* = 7.5 Hz, 1 H, Ar*H*) and 4.08 (s, 6 H, -OC*H*$_3$) ppm; ^{13}C NMR (400 MHz, CDCl$_3$) δ: 189.22, 161.49, 156.13, 152.01, 151.30, 136.75, 128.58, 126.33, 123.06, 125.37, 123.23, 121.47, 112.43, 110.47, 56.37 and 56.35 ppm. MS (ESI) *m/z*: Calcd for C$_{16}$H$_{13}$NO$_3$S, 299.1, Found 300.1 [M + H]$^+$.

4.4. Synthetic of intermediate 3

A solution of intermediate **2** (1.05 g, 3.51 mmol) in dry CH$_2$Cl$_2$ (50 mL) was cooled to -30 °C under an N$_2$ atmosphere. Then 14 mL BBr$_3$ (14.04 mmol) was slowly added to the cold solution. The mixture was stirred at -30 °C for 1h, and then at room temperature for another 24h. 70 mL water was added to the reaction and stirring continued for 2h. The reaction solution was extracted with ethyl acetate (100 mL × 3) three times,

washed with water, and dried with anhydrous Mg$_2$SO$_4$. The organic solvent was removed by evaporation and the crude residue was further purified by silica gel chromatography using *n*-hexane/CH$_2$Cl$_2$ (6/4, v/v) as eluent affording 0.42 g of yellow powder **3** (44.1 % yield). m.p. 214.3 ~ 215.5 °C. ^{1}H NMR (500 MHz, CDCl$_3$) δ: 12.09 (s, 1 H, -O*H*), 10.37 (s, 1 H, -C*H*O)，9.93 (s, 1 H, -O*H*), 8.07 (d, *J* = 8.5Hz, 1H, Ar*H*)，7.97 (d, *J*=8.0Hz,1H, Ar*H*), 7.57 (t, *J* = 7.5Hz, 1 H, Ar*H*), 7.50 (t, *J* = 8.0Hz, 1 H, Ar*H*)，7.36 (s, 1H, Ar*H*) and 7.32 (s, 1H, Ar*H*) ppm; ^{13}C NMR (500 MHz, CDCl$_3$) δ: 196.02, 167.35, 153.14, 151.74, 150.58, 133.27, 127.15, 126.53, 123.57, 122.87, 122.60, 121.72, 121.30 and 115.97 ppm. MS (ESI) *m/z*: Calcd for C$_{10}$H$_{10}$O$_4$, 271.0, Found 270.3[M-H]$^+$.

4.5. Synthesis of target fluorescent probe L

A mixture of intermediate **3** (130mg, 0.48mmol) and tris(2-aminoethyl)amine (23.3mg, 0.16mmol) in dry ethanol (30 mL) was refluxed for 24h under an N$_2$ atmosphere. The solvent was removed by evaporation, and the residue was recrystallized from methanol to afford 110 mg of a yellow solid **L** in 76 % yield. m.p. 264.4 ~ 265.3 °C. IR (KBr, vcm^{-1}): 3420 (OH), 1626 (C=N), 1497 (C=C), 1193 (C-N), 772 (Ar-H), 618 (Ar-H); ^{1}H NMR (500MHz, CDCl$_3$) δ: 12.72 (br, 3 H, -O*H*×3), 11.62 (s, 3 H, -O*H*×3), 8.22(s, 3 H, -C*H*=N×3), 7.82(t, *J* = 4.5Hz, 3 H, Ar*H*), 7.57 (t, *J* = 4.5Hz, 3 H, Ar*H*)，7.33 (m, 6 H, Ar*H*)，7.11 (s, 3 H, Ar*H*)，6.75 (s, 3 H, Ar*H*)，3.69 (t, *J* = 5.0Hz, 6 H, -N=C*H*$_2$CH$_2$×3) and 2.93 (t, *J* = 5.0Hz, 6 H, -N=CH$_2$C*H*$_2$×3) ppm; ^{13}C NMR (500 MHz, DMSO-*d*$_6$:CDCl$_3$) δ: 168.46, 165.46, 152.55, 151.70, 149.97, 133.04, 126.36, 125.45, 122.15, 122.00, 121.35, 119.46, 118.90, 114.69, 57.51 and 54.72 ppm. MS (MALDI-TOF) *m/z*: Calcd for C$_{48}$H$_{39}$N$_7$O$_6$S$_3$, 905.212, Found 906.322 [M+H]$^+$.

4.6. Spectral measurements

The recognition properties of probe **L** toward various metal ions (Li$^+$, Na$^+$, K$^+$, Mg^{2+}, Ca^{2+}, Ba^{2+}, Sr^{2+}, Cr^{3+}, Al^{3+}, Co^{2+}, Ni^{2+}, Cu^{2+}, Pb^{2+}, Cd^{2+}, Ag$^+$, Hg^{2+}, Fe^{3+}, Mn^{2+}, Zn^{2+}) were investigated by fluorescence spectroscopy in different media. To a 10 mL volumetric flask containing different metal ions, for Cr^{3+}, Al^{3+}, Zn^{2+}, diluted with DMF/H$_2$O (96/4, v/v) mixed solvent to 10 mL; for F$^-$, diluted with 1,4-dioxane to 10 mL, then the fluorescence sensing of ions was conducted. Fluorescence spectra were measured after 0 min (for F$^-$ in 1,4-Dioxane medium) or 45 min. (for Cr^{3+}, Al^{3+}, Zn^{2+} in 96:4 DMF/H$_2$O medium) upon addition of ions at room temperature to equilibrium. Fluorescence measurements were carried out with an excitation and emission slit width of 5 nm.

4.7. Cell culture and fluorescence imaging

PC3 cells were grown using a Roswell Park Memorial Institute 1640 supplemented with 10% fetal bovine serum, 1 IU/mL penicillin and 1 IU/mL streptomycin at 37 ℃ and 5% CO$_2$. One day prior to imaging, the cells were seeded in 12-well flat-bottomed plates. The next day, the cells were incubated with 20 μM of probe **L** for 65 min. (in 2% DMF) at 37 ℃. Before incubating with Al^{3+}(100μM) for another 50 min., Cr^{3+}(100μM) for another 45 min. and Zn^{2+} (100 μM)

for 60 min., respectively. The cells were rinsed with fresh culture medium containing phosphate-buffered saline (PBS) three times to remove the remaining probe, then fluorescent images of intracellular Al^{3+}, Cr^{3+} and Zn^{2+} were collected with an eclipse Ti-U (Nikon, Japan) inverted fluorescence microscope.

4.8. Determination of cytotoxicity by MTT assay

Cell viability was determined by using MTT (3-(4,5-dimethylthiazol-2-yl)-2,5-diphenyltetrazolium bromide) assays (Sigma-Aldrich). Breast cancer cell lines MCF-7 were plated in a 96-well plate at a concentration of $1{\times}10^5$ cells per well. The cells were treated with different concentrations of probe **L** (0, 10, 50, 100 and 500μM) for about 60 min. in a humidified incubator at 37 °C, 5% CO_2. 20μL MTT solution was added to each well of the plate, followed by incubation at 37 °C for 4 h. The supernatants were then aspirated carefully, and the formazan product was dissolved with 150 μL dimethyl sulfoxide. The absorbance was measured at a wavelength of 630 nm with a microplate reader (Multiskan GO，Thermo, USA).

Acknowledgements

Notes and references

1   (a) J. Li, D. Yim, W. D. Jang and J. Yoon, *Chem. Soc. Rev.*, 2017, **46**, 2437–2458. (b) H. S. Jung, P. Verwilst, W. Y. Kim and J. S. Kim, *Chem. Soc. Rev.*, 2016, **45**, 1242–1256.
2   (a) U. Panda, S. Roy, D. Mallick, A. Layek, P. P. Ray and C. Sinha, *J. Luminescence*, 2017, **181**, 56–62. (b) X. Liu, S. Liu and G. Liang, *Analyst*, 2016, **141**, 2600–2605. (c) J. F. Zhang, S. Kim, J. H. Han, S.-J. Lee, T. Pradhan, Q. Y. Cao, S. J. Lee, C. Kang and J. S. Kim, *Org. Lett.*, 2011, **13**, 5294-5297.
3   (a) P. Hou, S. Chen, H. Wang, J. Wang, K. Voitchovsky, X .Song. *Chem. Commun.*, 2014, **50**, 320–322. (b) S. Chen, H. Li and P. Hou, *Tetrahedron*, 2017, **73**, 589–593.
4   (a) J. Fan, M. Hu, P. Zhan, X. Peng, *Chem. Soc. Rev.*, 2013, **42,** 29–43. (b) J.-L. Zhao, H. Tomiyasu, C. Wu, H. Cong, X. Zeng, S. Rahman, P. E. Georghiou, D. L. Hughes, C. Redshaw and T. Yamato, *Tetrahedron*, 2015, **71**, 8521–8527. (c) X. Jia, Q. Chen, Y. Yang, Y. Tang, R. Wang, Y. Xu, W. Zhu, X. Qian, *J. Am. Chem. Soc.*, 2016, **138**, 10778–10781. (d) J. F. Zhang, C. S. Lim, S. Bhuniya, B. R. Cho and J. S. Kim, *Org. Lett.*, 2011, **13**, 1190-1193.
5   (a) C. Yang, Y. Chen, K. Wu, T. Wei, J. Wang, S. Zhang and Y. Han, *Anal. Methods*, 2015, **7**, 3327–3330. (b) D. Zhang, J.

Liu, H. Yin, H. Wang, S. Li, M. Wang, M. Li, L. Zhou, J. Zhang, *J Fluoresc*, 2016, **26**, 1367–1372; (c) B. Gu, L. Huang, W. Su, X. Duan, H. Li and S. Yao, *Anal. Chim. Acta.*, 2017, **954**, 97–104.
6   (a) Z. Huang, S. Ding, D. Yu, F. Huang, G. Feng, *Chem. Commun.*, 2014, **50**, 9185–9187. (b) Y. Zhou, X. He, H. Chen, Y. Wang, S. Xiao, N. Zhang, D. Li and K. Zheng, *Sensors and Actuators B: Chem.*, 2017, **247**, 626–631.
7   (a) X. Liu, Q. Yang, W. Chen, L. Mo, S. Chen, J. Kang and X. Song, *Org Biomol Chem.*, 2015, **13**, 8663–8668. (b) J. Wang, Y. Li, N. G. Patel, G. Zhang, D. Zhou and Y. Pang, *Chem. Commun.*, 2014, **50**, 12258–12261.
8   (a) J. -S. Wu, W. -M. Liu, J. -C. Ge, H. -Y. Zhang and P. -F. Wang, *Chem. Soc. Rev.*, 2011, **40**, 3483–3495. (b) J.-S. Wu, W. -M. Liu, X. -Q. Zhuang, F. Wang, P. -F. Wang, S. -L. Tao, X. -H. Zhang, S. -K. Wu and S. -T. Lee, *Org. Lett.*, 2007, **9**, 33–36.
9   (a) J. -Z. Zhao, S. -M. Ji, Y. -H. Chen, H. -M. Guo and P. Yang, *Phys. Chem. Chem. Phys.*, 2012, **14**, 8803–8817. (b) J. -F. Wang, Y. -B. Li, N. G. Patel, G. Zhang, D. -M. Zhou and Y. Pang, *Chem. Commun.*, 2014, **50**, 12258–12261;(c) J. -F. Wang, Y. -B. Li, E. Duaha, S. Paruchuri, D. -M. Zhou and Y. Pang, *J. Mater. Chem. B*, 2014, **2**, 2008–2012.
10   (a) X. Zhang and J.-Y. Liu, *Dyes and Pigments*, 2016, **125**, 80–88. (b) X. Peng, Y. Wu, J. Fan, M. Tian and K. Han, *J. Org. Chem.*, 2005, **70**, 10524–10531.
11   (a) T. Gunnlaugsson, M. Glynn, G. M. Tocci, P. E. Kruger and F. M. Pfeffer, *Coord. Chem. Rev.*, 2006, **250**, 3094–3117. (b) A. K. Mahapatra, R. Maji, K. Maiti, S. S. Adhikari, C. Das Mukhopadhyay and D. Mandal, *Analyst*, 2014, **139**, 309–317. (c) S. -D. Liu, L. -W. Zhang, P. -P. Zhou, W. -Y. Zan, X. -J. Yao, J. -J. Yang and Y. Yang, *RSC Adv.*, 2015, **5**, 19983–19988.